



Title	Activation cross sections of dysprosium-157,159 and terbium-160 radioisotopes from the deuteron-induced reactions on terbium-159 up to 24 MeV
Author(s)	Ichinkhorloo, Dagvadorj; Aikawa, Masayuki; Zolbadral, Tsoodol; Komori, Yukiko; Haba, Hiromitsu
Citation	Nuclear Instruments and Methods in Physics Research Section B : Beam Interactions with Materials and Atoms, 461, 102-104 <a href="https://doi.org/10.1016/j.nimb.2019.09.037">https://doi.org/10.1016/j.nimb.2019.09.037</a>
Issue Date	2019-09-27
Doc URL	<a href="http://hdl.handle.net/2115/82736">http://hdl.handle.net/2115/82736</a>
Rights	©2019 This manuscript version is made available under the CC-BY-NC-ND 4.0 license <a href="http://creativecommons.org/licenses/by-nc-nd/4.0/">http://creativecommons.org/licenses/by-nc-nd/4.0/</a>
Rights(URL)	<a href="https://creativecommons.org/licenses/by-nc-nd/4.0/">https://creativecommons.org/licenses/by-nc-nd/4.0/</a>
Type	article (author version)
File Information	NUCL INSTRUM METH B461_102-104.pdf



[Instructions for use](#)

Activation cross sections of dysprosium-157,159 and terbium-160 radioisotopes from the  
deuteron-induced reactions on terbium-159 up to 24 MeV

Dagvadorj Ichinkhorloo<sup>1,2\*</sup>, Masayuki Aikawa<sup>1,3</sup>, Tsoodol Zolbadral<sup>2,3</sup>,  
Yukiko Komori<sup>4</sup>, Hiromitsu Haba<sup>4</sup>

<sup>1</sup> Faculty of Science, Hokkaido University, Sapporo 060-0810, Japan

<sup>2</sup> Nuclear Research Center, National University of Mongolia, Ulaanbaatar 13330, Mongolia

<sup>3</sup> Graduate School of Biomedical Science and Engineering, Hokkaido University, Sapporo 060-8638,  
Japan

<sup>4</sup> Nishina Center for Accelerator-Based Science, RIKEN, Wako 351-0198, Japan

## Abstract

Experimental production cross sections of the deuteron-induced reactions on terbium-159 up to 24 MeV were measured. The stacked foil technique, the activation method and the  $\gamma$ -ray spectrometry were used for the measurement. The production cross sections of <sup>157,159</sup>Dy and <sup>160</sup>Tb were determined and compared with the experimental data studied earlier and the theoretical calculation.

## Keyword

Dysprosium-157; Dysprosium-159; Terbium-160; Deuteron irradiation; Terbium target; Excitation function; Cross section

## 1. Introduction

The radioisotopes dysprosium-157 ( $T_{1/2} = 8.14$  h) and dysprosium-159 ( $T_{1/2} = 144.4$  d) can be used for bone scanning (Skeletal imaging) [1] and determination of bone mineral [2], respectively. The dysprosium radionuclides can be produced by charged-particle-induced reactions on a mono isotopic element target of terbium-159. In this work, the production cross sections of <sup>157,159</sup>Dy and <sup>160</sup>Tb in the deuteron-induced reactions were studied. The results were compared with the experimental data published earlier [3–5] and the TENDL-2017 data [6] based on calculation using the theoretical model code TALYS.

## 2. Experimental

A 24-MeV deuteron beam was extracted from the RIKEN AVF cyclotron. The stacked foil

---

\* Corresponding author: [ichinkhorloo@nucl.sci.hokudai.ac.jp](mailto:ichinkhorloo@nucl.sci.hokudai.ac.jp)

technique, the activation method and the high-resolution  $\gamma$ -ray spectrometry were used to determine the activation cross sections.

The stacked target foils of each  $10 \times 10 \text{ mm}^2$  were cut from a large Tb foil ( $25 \times 50 \text{ mm}^2$ , 99.9% purity, Nilaco Corp., Japan) and two Ti foils ( $50 \times 100 \text{ mm}^2$ , 99.6% purity and  $120 \times 100 \text{ mm}^2$ , 99.5% purity, Nilaco Corp., Japan). The sizes and weights of the large Tb and Ti foils were measured to derive the thicknesses of 20.56, 2.25 and  $9.31 \text{ mg/cm}^2$ , respectively. The stacked target consisted of 17 sets of Tb-Ti-Ti foils with one thin Ti foil at the top. The second Ti foils of the sets were used to confirm the beam parameters and target thicknesses using the  ${}^{\text{nat}}\text{Ti}(d,x){}^{48}\text{V}$  monitor reaction. The thin Ti foil with a small reduction of the projectile energy was only inserted at the top to double-check the incident energy. The Tb foils were measured with the next Ti foils to take recoil products into account. The stacked target was put into the target holder which was served as a Faraday cup.

The deuteron beam was accelerated to 23.9 MeV by the RIKEN AVF cyclotron. The beam energy was measured by the time-of-flight method [7]. The stacked target was irradiated by the beam for 60 min with an average intensity of 94.3 nA. The beam intensity was measured by the Faraday cup. Energy degradation in the stacked target was calculated using the SRIM code [8].

The  $\gamma$ -rays emitted from the irradiated foils were measured by a high-resolution HPGe detector (ORTEC GEM30P4-70). The detector was calibrated by a standard  $\gamma$ -ray source composed of  ${}^{57,60}\text{Co}$ ,  ${}^{88}\text{Y}$ ,  ${}^{109}\text{Cd}$ ,  ${}^{113}\text{Sn}$ ,  ${}^{137}\text{Cs}$ ,  ${}^{139}\text{Ce}$  and  ${}^{241}\text{Am}$ . The  $\gamma$ -ray spectra were analyzed by the software Gamma Studio (SEIKO EG&G). Reaction and decay data for the  $\gamma$ -ray spectrometry were taken from NuDat 2.7 [9], Lund/LBNL Nuclear Data Search [10], LiveChart [11] and QCalc [12] and summarized in Table 1.

Table 1. Reactions and decay data of reaction products [9–12]

Nuclide	Half-life	Decay mode (%)	$E_\gamma$ (keV)	$I_\gamma$ (%)	Contributing reactions	Q-value (MeV)
${}^{159}\text{Dy}$	144.4 d	$\varepsilon$ : (100)	58.0	2.27(13)	${}^{159}\text{Tb}(d,2n)$	-3.372
${}^{157}\text{Dy}$	8.14 h	$\varepsilon$ : (100)	326.336	93(3)	${}^{159}\text{Tb}(d,4n)$	-19.257
${}^{160}\text{Tb}$	72.3 d	$\beta^-$ : (100)	298.5783	26.1(6)	${}^{159}\text{Tb}(d,p)$	4.150

The self-absorption of low energy  $\gamma$ -rays in the Tb foils were considered using the following formula [13]

$$A(E) = A_0(E) \frac{\rho[\mu(E)/\rho]d}{1 - \exp[-\rho(\mu(E)/\rho)d]}, \quad (1)$$

where  $A_0(E)$  is the measured activity for the  $\gamma$ -ray at the energy  $E$ ,  $A(E)$  is the corrected activity,  $d$  is the thickness of the Tb foil,  $\rho$  is the density of the foil,  $\mu(E)/\rho$  is the mass attenuation coefficient for the  $\gamma$ -ray at the energy  $E$  taken from [14].

### 3. Result and discussion

The cross sections of the  $^{nat}\text{Ti}(d,x)^{48}\text{V}$  monitor reaction were derived using the  $\gamma$  line at 983.525 keV ( $I_\gamma = 99.98\%$ ). The derived cross sections were compared with the recommended values from IAEA [15]. Based on the comparison, the measured beam intensity was corrected by decreasing 4.7%. The corrected cross sections of the monitor reaction are shown in Fig. 1. We could obtain good agreements between the results and the recommended values.

Production cross sections of  $^{157,159}\text{Dy}$  and  $^{160}\text{Tb}$  in the deuteron-induced reactions on  $^{159}\text{Tb}$  were determined. The numerical data are tabulated in Table 2 and graphically shown in Figs. 2-4 in comparison with the previous data [3–5] and the TENDL-2017 data [6]. The total uncertainties (9.0-12.5%) were estimated from the square root of the quadratic summation of each component; statistical uncertainty (0.4-7.0%), target thickness (2%), target purity (1%), beam intensity (5%), detector efficiency (6%),  $\gamma$ -ray intensity (2.3-5.7%) and peak fitting (3%).

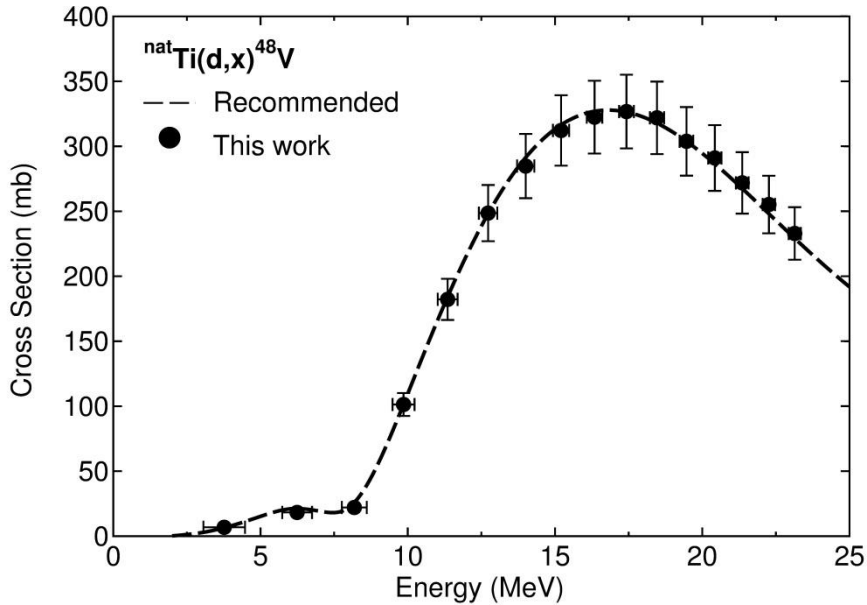


Fig. 1. Excitation function of the  $^{nat}\text{Ti}(d,x)^{48}\text{V}$  monitor reaction with the recommended values [15].

Table 2. Production cross sections obtained in the experiment

Energy (MeV)	$^{159}\text{Tb}(d,2n)^{157}\text{Dy}$ (mb)	$^{159}\text{Tb}(d,4n)^{159}\text{Dy}$ (mb)	$^{159}\text{Tb}(d,p)^{160}\text{Tb}$ (mb)
23.7±0.2	122.5±11.3	149.3±16.7	84.9±7.5
22.8±0.2	50.0±4.6	169.6±18.2	86.4±7.8
21.9±0.2	11.8±1.1	170.9±18.4	91.7±8.2
21.0±0.2	1.0±0.1	187.0±20.1	97.4±8.7
20.1±0.2		222.4±23.6	105.5±9.5

19.1±0.2	262.8±27.8	115.6±10.4
18.1±0.3	306.3±32.3	122.8±11.0
17.0±0.3	407.4±42.8	140.7±12.6
15.9±0.3	460.3±48.3	146.7±13.2
14.8±0.3	592.6±61.9	164.6±14.8
13.6±0.3	662.3±69.1	185.9±16.7
12.3±0.3	604.0±63.1	188.1±16.9
10.8±0.4	477.0±50.0	200.3±18.0
9.3±0.4	237.8±25.2	157.4±14.1
7.5±0.5	47.2±5.66	59.1±5.3
5.5±0.6		4.4±0.4
2.6±1.1		1.1±0.1

### 3.1 The $^{159}\text{Tb}(d,2n)^{159}\text{Dy}$ reaction

The  $\gamma$  line at 58.0 keV ( $I_\gamma = 2.27\%$ ) from the  $^{159}\text{Dy}$  decay ( $T_{1/2} = 144.4$  d) was measured to derive the cross sections of the  $^{159}\text{Tb}(d,2n)^{159}\text{Dy}$  reaction. The measurements were performed after a cooling time of 94 days. The  $\gamma$  line had negligible interference with the x-ray of the lead shielding of the detector, which could be confirmed by no peaks found at the energy in the two foils at the downstream of the beam. The mass attenuation coefficient adopted for the  $\gamma$  line at 58.0 keV was  $13.6 \text{ cm}^2/\text{g}$  [14]. The correction factor calculated from Eq. (1) for the  $\gamma$  line is 1.15. The corrected activities were the product of the measured net counts and the correction factor. The cross sections derived from the corrected activities for the  $^{159}\text{Dy}$  production are presented with the previous experimental data [3,5] and the TENDL-2017 data [6] in Fig. 2. Our experimental data have a peak at around 14 MeV, which are the same as other experimental data while the amplitudes are largely different. The peak amplitude of the TENDL-2017 data agrees with our data although its position is slightly deviate to lower energy from ours. The TENDL-2017 data overestimate all the experimental data between 18 MeV and 35 MeV.

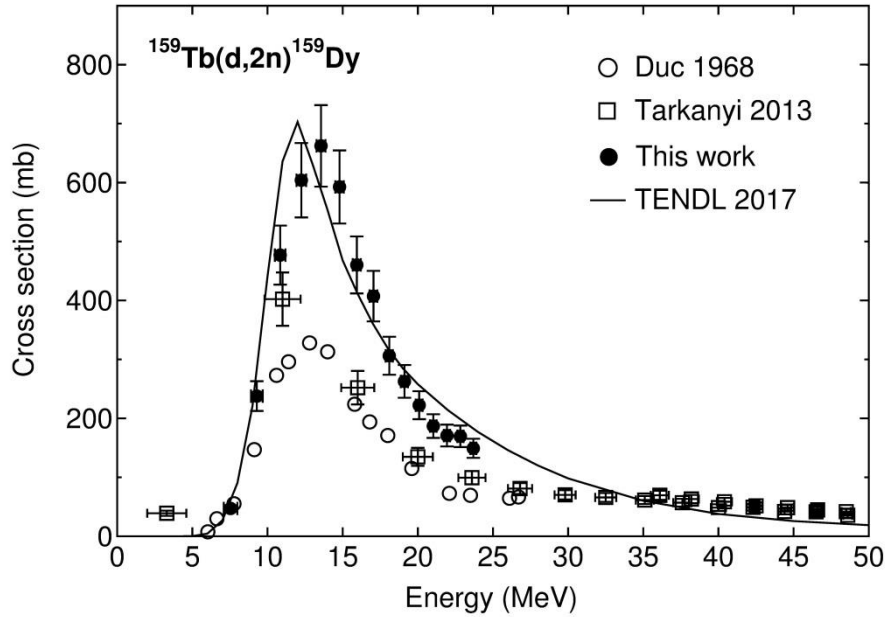


Fig. 2. Excitation function of the  $^{159}\text{Tb}(d,2n)^{159}\text{Dy}$  reaction

### 3.2 The $^{159}\text{Tb}(d,4n)^{157}\text{Dy}$ reaction

The excitation function of the  $^{159}\text{Tb}(d,4n)^{157}\text{Dy}$  reaction was determined based on the  $\gamma$  line at 326.336 keV ( $I_\gamma = 93.0\%$ ) from the decay of  $^{157}\text{Dy}$  ( $T_{1/2} = 8.14$  h). The measurements after a cooling time of 21 hours were used to derive the cross sections. We could obtain only four experimental data points above 20 MeV due to the Q-value listed in Table 1. Our result is compared with the earlier data [3–5] and the TENDL-2017 data [6] as shown in Fig. 3. The data by Duc et al. [3] and Siri et al. [4] agree with our data, while the data by Tarkanyi et al. [5] show larger amplitude than ours at around 20 MeV. The TENDL-2017 data overestimate most of the experimental data up to 32 MeV except for the data by Tarkanyi et al. [5] below 20 MeV.

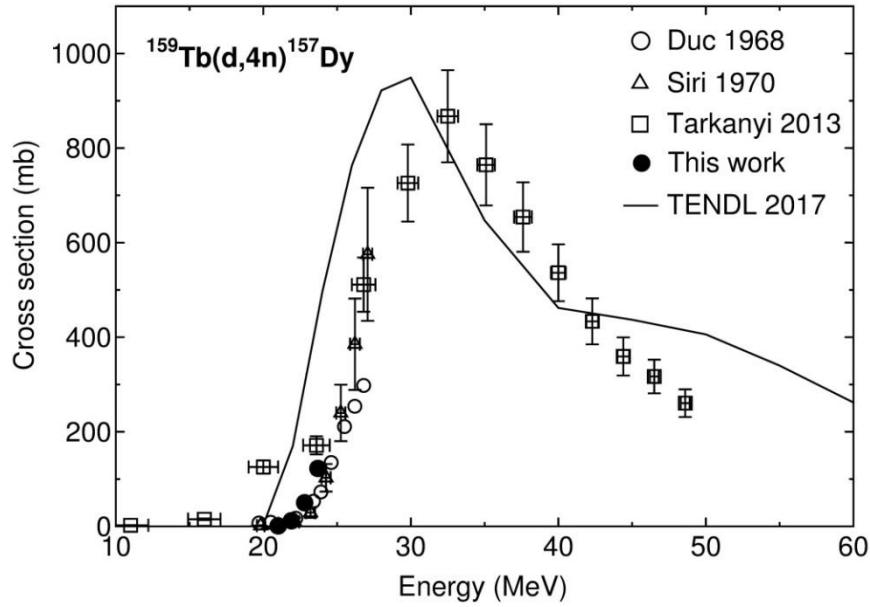


Fig. 3. Excitation function of the  $^{159}\text{Tb}(d,4n)^{157}\text{Dy}$  reaction

### 3.3 The $^{160}\text{Tb}(d,p)^{160}\text{Tb}$ reaction

The radionuclide  $^{160}\text{Tb}$  has the half-life of  $T_{1/2} = 72.3$  d. The measurements of the 298.57-keV  $\gamma$  line ( $I_{\gamma} = 26.1\%$ ) from the  $^{160}\text{Tb}$  decay were performed after a cooling time of 94 days. The derived cross sections are shown in Fig. 4 together with the earlier experimental data [3–5] and the TENDL-2017 data [6]. Our results show almost good agreement with the data by Tarkanyi et al. [5] in the energy region of our experiment. The TENDL-2017 data largely underestimate the two previous experimental data [4,5] and ours, although better agreement can be found with the data by Duc et al. [3].

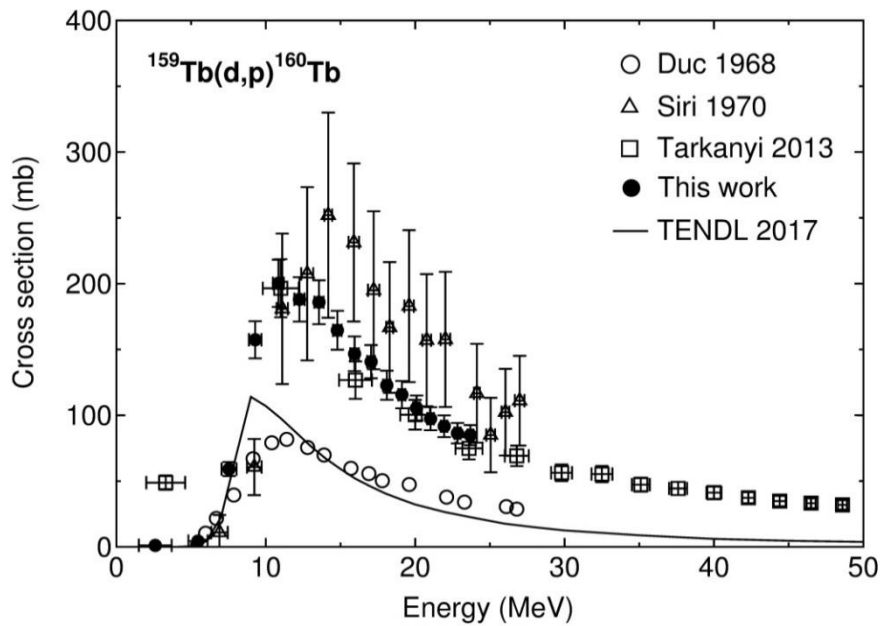


Fig. 4. Excitation function of the  $^{159}\text{Tb}(d,p)^{160}\text{Tb}$  reaction

#### 4. Summary

In the present work, we performed an experiment to measure the excitation functions of the deuteron-induced reactions on  $^{159}\text{Tb}$  up to 24 MeV at the RIKEN AVF cyclotron. The stacked foil technique, the activation method and the high-resolution  $\gamma$ -ray spectrometry were used. The production cross sections of  $^{157,159}\text{Dy}$  and  $^{160}\text{Tb}$  were determined. The results are compared with the experimental data studied earlier and the TENDL data using the theoretical model code TALYS. We can find acceptable agreement between our results and some of the previous experimental results.

#### Acknowledgement

This work was carried out at RI Beam Factory operated by RIKEN Nishina Center and CNS, University of Tokyo, Japan. This work was supported by JSPS KAKENHI Grant Number 17K07004.

#### Declarations of interest

None

#### References

- [1] G. Subramanian, J.G. McAfee, R.J. Blair, R.E. O'Mara, M.W. Greene, E. Lebowitz,  $^{157}\text{Dy}$ -HEDTA for skeletal imaging., *J. Nucl. Med.* 12 (1971) 558–61. <http://www.ncbi.nlm.nih.gov/pubmed/4999219> (accessed July 8, 2019).

- [2] D. V. Rao, G.F. Govelitz, K.S.R. Sastry, Dysprosium 159 for transmission imaging and bone mineral analysis, *Med. Phys.* 4 (1977) 109–114. doi:10.1118/1.594307.
- [3] T.M. Duc, J. Tousset, M.F. Perrin, Excitation function of reactions induced on terbium by 26.9 MeV deuterons, *C. R. Acad. Sci. Ser. B.* 266 (1968) 100–102.
- [4] L.N.Siri and S.J.Nassiff, Excitation Functions for  $^{159}\text{Tb}(d,p)^{159}\text{Tb}$  and  $^{160}\text{Tb}(d,4n)^{157}\text{Dy}$  Reactions, *Radiochim. Acta.* 14 (1970) 159–160. doi:10.1524/ract.1970.14.34.159.
- [5] F. Tárkányi, S. Takács, F. Ditrói, A. Hermanne, A. V. Ignatyuk, Activation cross-sections of longer-lived radioisotopes of deuteron induced nuclear reactions on terbium up to 50 MeV, *Nucl. Instruments Methods Phys. Res. Sect. B Beam Interact. with Mater. Atoms.* 316 (2013) 183–191. doi:10.1016/j.nimb.2013.09.008.
- [6] A.J. Koning, D. Rochman, J.C. Sublet, N. Dzysiuk, M. Fleming, S. van der Marck, TENDL: Complete Nuclear Data Library for Innovative Nuclear Science and Technology, *Nucl. Data Sheets.* 155 (2019) 1–55. doi:10.1016/j.nds.2019.01.002.
- [7] K.Y. T. Watanabe, M. Fujimaki, N.Fukunishi, H. Imao, O.Kamigaito, M. Kase, M.Komiyama, N. Sakamoto, K.Suda, M.Wakasugi, Beam energy and longitudinal beam profile measurement system at the RIBF, *Proc. 5th Int. Part. Accel. Conf. (IPAC 2014).* (2014) 3566–3568.
- [8] J.F. Ziegler, J.P. Biersack, M.D. Ziegler, *SRIM: the Stopping and Range of Ions in Matter*, (2008). <http://www.srim.org>.
- [9] National Nuclear Data Center, Nuclear structure and decay data on-line library, *Nudat 2.7*, (2017). <http://www.nndc.bnl.gov/nudat2/>.
- [10] S.Y.F. Chu, L.P. Ekström, R.B. Firestone, The Lund/LBNL Nuclear Data Search, <http://nucleardata.nuclear.lu.se/toi/>.
- [11] International Atomic Energy Agency, LiveChart of Nuclides, (2009). <https://www-nds.iaea.org/livechart/>.
- [12] B. Pritychenko, A. Sonzogni, Q-value Calculator (QCalc), (2003). <http://www.nndc.bnl.gov/qcalc/>.
- [13] Z.B. Alfassi, E. Persico, F. Groppi, M.L. Bonardi, On the photon self-absorption correction for thin-target-yields vs . thick-target-yields in radionuclide production, *Appl. Radiat. Isot.* 67 (2009) 240–242. doi:10.1016/j.apradiso.2008.10.004.
- [14] Photon Interaction Database, National Institute of Standards and Technology, <https://physics.nist.gov/PhysRefData/XrayMassCoef/tab3.html>.
- [15] A. Hermanne, A. V. Ignatyuk, R. Capote, B. V. Carlson, J.W. Engle, M.A. Kellett, T. Kibédi, G. Kim, F.G. Kondev, M. Hussain, O. Lebeda, A. Luca, Y. Nagai, H. Naik, A.L. Nichols, F.M. Nortier, S. V. Suryanarayana, S. Takács, F.T. Tárkányi, M. Verpelli, Reference Cross Sections for Charged-particle Monitor Reactions, *Nucl. Data Sheets.* 148 (2018) 338–382. doi:10.1016/j.nds.2018.02.009.